Adsorptive Stripping Voltammetry of Hen-Egg-White-Lysozyme via Adsorption-Desorption at an Array of Liquid-Liquid Microinterfaces

ARTICLE *in* ANALYTICAL CHEMISTRY · MARCH 2012

Impact Factor: 5.64 · DOI: 10.1021/ac203249p · Source: PubMed

2 AUTHORS:

Eva Alvarez de Eulate
Curtin University
12 PUBLICATIONS **65** CITATIONS
SEE PROFILE

Damien W M Arrigan
Curtin University
158 PUBLICATIONS **3,159** CITATIONS
SEE PROFILE

analytical chemistry

Article

pubs.acs.org/ac

Adsorptive Stripping Voltammetry of Hen-Egg-White-Lysozyme via Adsorption−Desorption at an Array of Liquid−Liquid Microinterfaces

Eva Alvarez de Eulate and Damien W. M. Arrigan*

Nanochemistry Research Institute, Department of Chemistry, Curtin University, GPO Box U1987, Perth, WA 6845, Australia

Supporting Information

ABSTRACT: Electrochemical adsorption and voltammetry of hen-egg-white-lysozyme (HEWL) was studied at an array of microinterfaces between two immiscible electrolyte solutions (μITIES). Adsorption of the protein was achieved at an optimal applied potential of 0.95 V, after which it was desorbed by a voltammetric scan to lower potentials. The voltammetric peak recorded during the desorption scan was dependent on the adsorption time and on the aqueous phase concentration of HEWL. The slow approach to saturation or equilibrium indicated that protein reorganization at the interface was the rate-determining step and not diffusion to the interface. For higher concentrations and longer adsorption times, a HEWL multilayer surface coverage of 550 pmol cm^{-2} was formed, on the basis of the assumption that a single monolayer corresponded to a surface coverage of 13 pmol cm^{-2}. Implementation of adsorption followed by voltammetric detection as an adsorptive stripping voltammetric approach to HEWL detection demonstrated a linear dynamic range of 0.05−1 μM and a limit of detection of 0.03 μM, for 5 min preconcentration in unstirred solution; this is a more than 10-fold improvement over previous HEWL detection methods at the ITIES. These results provide the basis for a new analytical approach for label-free protein detection based on adsorptive stripping voltammetry.

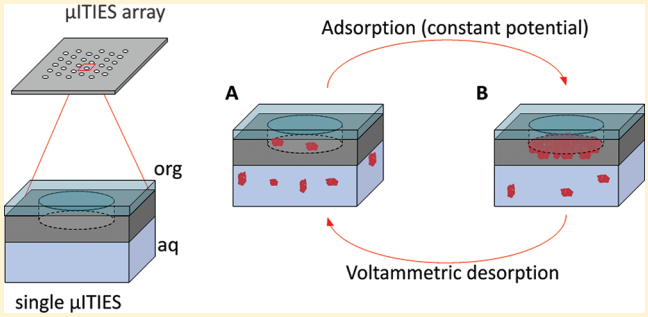

Proteins are essential components of organisms and participate directly or indirectly in every process within a biological cell. The understanding and control of the fundamental processes in which proteins are involved is of great importance and may lead to new applications in biomedical diagnostics and therapy.[1]

Lysozyme is a compact globular protein consisting of 129 amino acid residues stabilized by four cysteine disulfide bonds.[2,3] Hen-egg-white lysozyme (HEWL) possesses a molecular weight of ∼14 600 g mol^{-1}[4] and has an ellipsoid structure.[5] At physiological pH, HEWL is positively charged due to its isoelectric point (pI) of 11.35.[6] The primary function of lysozyme is to promote the hydrolysis of polysaccharides in the cell walls of Gram-positive bacteria.[7] It is present in mucosal secretions such as saliva, mucus, tears, and human milk.[8] Increased levels of lysozyme can be used as indicators of some diseases, for instance Crohn's disease,[9] breast cancer,[10] gastric cancer,[11] leukemia, and meningitis.[12] In contrast, some studies have suggested that lysozyme has potential in HIV treatment[13] and as an anticancer drug.[14]

Electrochemistry at the interface between two immiscible electrolyte solutions (ITIES), or at the liquid−liquid interface,[15−18] has been shown to offer an excellent capability for label-free biomolecular detection and quantification. Over the past 30 years, bioactive molecules such as neurotransmitters, carbohydrates, drugs, peptides, and DNA have been studied at the ITIES.[19] Amemiya et al. have reported the transfer of the highly charged polypeptide protamine across the water/1,2-dichloroethane interface.[20] Facilitated transfer of amino acids[21] and peptides[21,22] in the presence of dibenzo-18-crown-6-ether (DB18C6) has been used as a method for their detection. Vagin and co-workers reported the spontaneous formation of micelles at polarized interfaces and used these as carriers to transfer proteins into the organic phase[23,24] while Osakai et al. have recently studied the effect of surfactants and micelle formation at the water/oil interface in the presence of polypeptides and proteins including protamine, lysozyme, albumin, myoglobin, and alpha-lactalbumin.[25,26] They have suggested that adsorption is dependent on the relative densities of charged, polar, and nonpolar regions of the protein.[26] HEWL has already been subjected to a number of studies at the ITIES. Scanlon et al. studied its electrochemical behavior at the ITIES and demonstrated adsorption at both liquid ITIES and at gel-supported microinterfaces between two immiscible electrolyte solutions (μITIES) array. The detection mechanism was proposed to involve protein adsorption in its cationic state at the ITIES and facilitated transfer of organic phase anion across the ITIES to form a complex with the protein on the aqueous side of the interface,[27,28] as suggested for protamine by Samec et al.[29] The interfacial formation of complexes of lysozyme and hydrophobic anions was recently confirmed using an online

Received: December 13, 2011
Accepted: January 14, 2012
Published: January 15, 2012

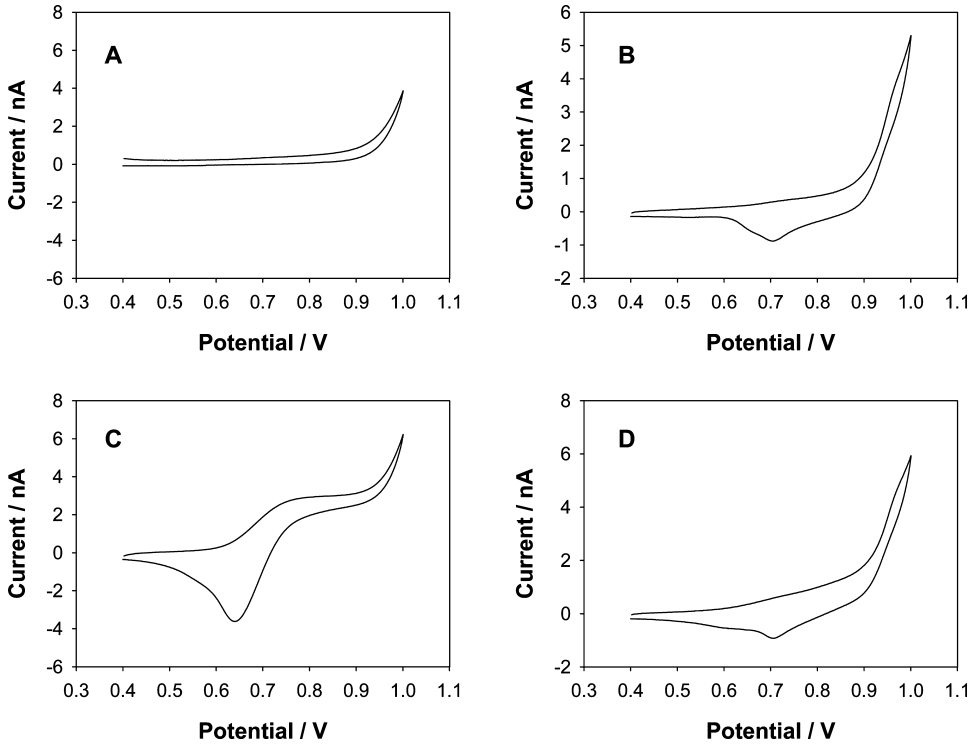

Figure 1. Cyclic voltammetry of the μITIES array in the absence and presence of aqueous phase HEWL and TEA^+: (A) aqueous phase, 10 mM HCl; (B) aqueous phase, 15 μM HEWL + 10 mM HCl; (C) aqueous phase, 15 μM TEA^+ + 10 mM HCl; (D) aqueous phase: 15 μM HEWL + 15 μM TEA^+ + 10 mM HCl. In all cases, the organic phase was as described in Scheme S-1, Supporting Information. Scan rate for all experiments: 5 mV s^{-1}.

mass spectrometry approach by Hartvig et al.[30] Other proteins and polypeptides were seen to undergo a similar detection mechanism at the ITIES, such as hemoglobin[31,32] and insulin.[33] In the case of hemoglobin, multilayer adsorption at the ITIES was suggested and independent evidence for the interaction of cationic hemoglobin with hydrophobic anions was obtained using acoustic sensor technology.[34]

To date, the detection limits for proteins based on voltammetric detection at the ITIES have been in the low micromolar range, with one report of the detection of 0.5 μM HEWL[28] using background-subtracted cyclic voltammetry at a μITIES array. For detection in biomedical areas, such as in disease diagnostics,[35] lower detection limits are needed. In voltammetric methods of analysis, a widely used strategy for improving detection limits is to preconcentrate the target analyte onto or into the working electrode surface prior to the voltammetric measurement. This approach is referred to as stripping voltammetry, with variants such as anodic, cathodic, adsorptive, abrasive, and catalytic adsorptive stripping voltammetry.[36,37] The use of adsorption as a preconcentration step has been widely studied for detection of organic, inorganic, and biological molecules[38] at especially mercury electrodes via the method of adsorptive stripping voltammetry (AdSV). A prime example of the AdSV approach is the detection of trace nickel by its adsorptive preconcentration as a complex with dimethylglyoxime.[39] Such an approach was suggested by Amemiya and co-workers for detection of heparin, a mixture of sulphated carbohydrates, at a micropipet-based μITIES.[40]

Although the adsorption of proteins at the ITIES has been studied with various methods, examination of adsorptive accumulation as a way to improve protein detection limits has not been addressed. Consequently, the purpose of the work reported here is to examine the adsorption of HEWL at the ITIES, in this particular case at the gelled μITIES array, as a basis for preconcentration prior to voltammetric detection, and to assess any improvement in detection limits brought about by this adsorption.

EXPERIMENTAL SECTION

Reagents. All the reagents were purchased from Sigma-Aldrich Australia Ltd. and used as received unless indicated otherwise. The organic phase was gelled and prepared using bis(triphenylphosphoranylidene) tetrakis(4-chlorophenyl)-borate ($BTPPA^+TPBCl^-$, 10 mM) in 1,6-dichlorohexane (1,6-DCH) and low molecular weight poly(vinyl chloride) (PVC).[28,41] The $BTPPA^+TPBCl^-$ salt was prepared by metathesis of bis(triphenylphosphoranylidene)ammonium chloride ($BTPPA^+Cl^-$) and potassium tetrakis(4-chlorophenyl)borate (K^+TPBCl^-). Stock solutions of HEWL were prepared in 10 mM HCl of pH 2 on a daily basis. Tetraethylammonium (TEA^+) chloride was also dissolved in 10 mM HCl of pH 2. All the aqueous solutions were prepared in purified water, from a USF Purelab plus UV, with a resistivity of 18 MΩcm.

Apparatus. All experiments were performed using an AUTOLAB PGSTAT302N electrochemical analyzer (Metrohm, The Netherlands). The micropore arrays used to form the micro-ITIES array were fabricated in silicon.[42] The fabrication procedure provided hydrophobic micropore walls so that the organic phase filled the pores.[42,43] The micropore array consisted of 30 micropores arranged in a hexagonal close-packed arrangement, each with a diameter of 22.4 μm and a pore center-to-center distance of 200 μm. These microporuos silicon membranes were sealed onto the lower orifice of a glass cylinder using a silicone rubber (acetic acid curing Selleys glass silicone (Selleys Australia and New Zealand)). The gellified

dx.doi.org/10.1021/ac203249p | Anal. Chem. 2012, 84, 2505−2511

organic phase solution was introduced into the silicon micropore array via the glass cylinder,[44] and the organic reference solution was placed on top of the gellified organic phase. The silicon membrane was then immersed into the aqueous phase (10 mM HCl, HEWL in 10 mM HCl, and/or TEA^+ in 10 mM HCl). The electrochemical cell employed is summarized in Scheme S-1, Supporting Information. Contact angle measurements were performed with a contact angle goniometer (KSV Instruments LTP, Finland) on a glass slide spin-coated with a film of gellified organic phase.

Electrochemical Measurements. The interfacial potential difference was applied and measured between a pair of Ag/AgCl electrodes. The geometric area of the microinterfaces was 1.18×10^{-4} cm^2. Cyclic voltammetry (CV), linear sweep voltammetry (LSV), and linear sweep stripping voltammetry (LSSV) were carried out at a sweep rate of 5 mV s^{-1}, unless otherwise stated, and parameters such as protein concentration, applied potential, and duration of the adsorption stage were varied.

RESULTS AND DISCUSSION

Distortion of Simple Ion Transfer by Adsorption. A qualitative indication of whether a macromolecule is adsorbed at the μITIES can be obtained not only by examination of the CV of the macromolecule at the interface but also by comparison of the voltammetric response for a simple ion transfer process in the presence and absence of the macromolecule.[28,45] If the macromolecule is adsorbed at the μITIES, then the CV for simple ion transfer should be distorted, depending on the extent of adsorption. Figure 1 shows CVs for HEWL adsorption at the μITIES array. Figure 1A shows the background CV response, obtained when both phases contain only the background electrolyte species. The rise in current at the positive end of the voltammogram is indicative of background electrolyte transfer across the ITIES.[28] Figure 1B shows the situation when the aqueous phase contains 15 μM HEWL. There are differences between the CV in the presence and absence of HEWL, which indicates that HEWL can be detected, most easily by the reverse scan peak, which may be attributed to desorption of HEWL from the interface. The broad increase in current between ca. 0.6 and 0.9 V is due to the adsorption of HEWL at the interface but it is not useful for detection purposes because of its broadness. The response of HEWL at the ITIES is complex and, as discussed previously,[27,28,30] is a combination of HEWL adsorption at the interface and its facilitation of the transfer of background electrolyte anion from the organic phase to the aqueous phase where it forms a complex with the cationic protein. In contrast to the complex nature of HEWL detection, the transfer of TEA^+ (Figure 1C) is a simple ion transfer process dominated by mass transport: radial diffusion on the forward (positive-going) scan provides a steady-state voltammogram, and linear diffusion (in the micropores used to form the μITIES) on the reverse scan (negative-going) produces a peak-shaped response.[28] However, this ideal response to TEA^+ is severely distorted in the presence of aqueous phase HEWL (Figure 1D). Although a transfer current for TEA^+ can be discerned on the forward scan, it is smaller and less well-defined than that in the absence of HEWL (Figure 1C). A peak for the reverse transfer of TEA^+ can be seen at ca. 0.6 V. The peak at ca. 0.7 V is due to desorption of HEWL from the interface. Transfer of the TEA^+ from the aqueous phase to the organic phase in the presence of HEWL was distorted from the expected steady-state response for TEA^+ transfer across the interface. This behavior indicates an adsorbed protein layer is formed. The reverse sweep for TEA^+ in the presence of HEWL was affected also, despite apparent desorption of protein before the TEA^+ reverse peak potential. This is because the adsorbed protein results in a decreased concentration of TEA^+ for the reverse transfer in comparison to that in the absence of protein. Also, as discussed by Hartvig et al.,[30] adsorption of protein may occur at potentials positive of the potential of zero charge so that protein adsorption occurs over a wide potential range.

Potential-Dependent Adsorption of HEWL. The influence of applied potential on HEWL adsorption at the μITIES array was investigated by holding the applied potential at predetermined values for a certain time, followed by scanning to lower potentials in order to desorb the protein and produce a stripping voltammogram. The influence of the applied potential on HEWL adsorption is shown in Figure 2. Since

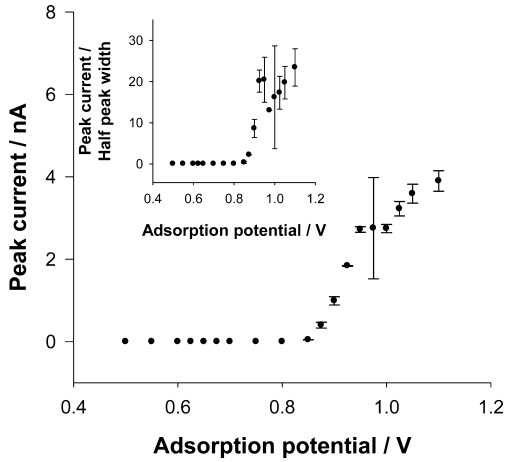

Figure 2. Influence of the applied potential during the adsorption step on the peak current and ratio of peak current/peak half-width. Concentration of HEWL: 10 μM in 10 mM HCl. Adsorption time: 60 s, without stirring. The organic phase was as described in Scheme S-1, Supporting Information.

the potential for protein adsorption was close to the region where background electrolyte transfer occurs, the optimum potential was assessed by examining both the peak current and the ratio of peak height: half-peak width for the desorption voltammogram. The optimum protein adsorption potential is a compromise between the maximum desorption current and the minimum background signal. The optimum adsorption potential was determined to be 0.95 V for HEWL. At this adsorption potential, the peak current reaches a shoulder but continues to rise at higher applied potentials (due to contributions from background electrolyte transfer). In contrast, the ratio of peak height/half-peak width reaches a plateau at this potential, indicating there is no added benefit to applying higher applied potentials during the adsorption process.

Interestingly, at potentials $\leq$0.8 V, the peak currents are low, indicating that the amount of HEWL adsorbed to the interface at these applied potentials is not high. This suggests that the simple ion transfer of TEA^+ (Figure 1C) should be evident at potentials $\leq$0.8 V. It may well be that the minute amounts of HEWL adsorbed at these potentials are sufficient to distort the TEA^+ transfer described above. Indeed, low surface coverages for protamine, a polypeptide of lower RMM than HEWL, were

dx.doi.org/10.1021/ac203249p | Anal. Chem. 2012, 84, 2505−2511

determined[30] in an equivalent potential region, where no charge transfer current was measured. Protamine surface coverages of ca. 8×10^{-11} mol cm^{-2}, consistent with a monolayer or so of this polypeptide, were found. Similar adsorption of a monolayer of HEWL in this potential region ($\leq$0.8 V) would also distort the TEA^+ voltammogram.

Scan Rate Dependence. Figure S-1, Supporting Information, shows voltammograms recorded at different scan rates, following adsorption at constant potential from unstirred solution. The shift in the stripping peak potential is attributed to the uncompensated resistance in the cell. The linear dependence of the desorption peak current on the scan rate is illustrated in the inset graph and is as expected for a charge transfer process involving an adsorbed species. Consequently, the peak current is directly proportional to the surface coverage (Γ) as well as the potential scan rate (υ), according to the equation:[46]

$$i_p = \frac{z_i^2 F^2 \Gamma A \upsilon}{4RT} \quad (1)$$

where i_p is the peak current, z_i is the number of charges transferred per molecule, F is the Faraday constant, R is the universal gas constant, T is the temperature, and A is the total interfacial area, 1.18×10^{-4} cm^2. At a temperature of 21 °C and assuming that the number of ions transferred per molecule is the same as the protein charge, +17,[47] the surface coverage obtained from the slope of the line of the inset graph in Figure S-1, Supporting Information, is 4 pmol cm^{-2}, for a 0.5 μM HEWL aqueous solution concentration and a 60 s adsorption time.

Time Dependence. Figure 3 shows the influence of adsorption time on the voltammetric desorption response.

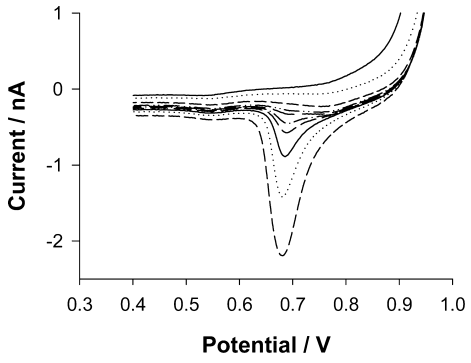

Figure 3. AdSV of 0.1 μM HEWL at different preconcentration times from 0 s (—) to 1800 s (- -) via times of 5, 60, 150, 180, 240, 300, 480, and 900 s.

Without any time for adsorption (i.e., 0 s adsorption), it was not possible to detect 0.1 μM HEWL in the aqueous phase. However, LSV following adsorption of HEWL at the μITIES for times longer than 60 s provided stripping peaks at this low concentration. Figure S-2, Supporting Information, indicates that after each desorption voltammogram, the protein is stripped away from the interface, so that there is no carryover between experiments.

The kinetics of the adsorption process was examined across a range of aqueous phase HEWL concentrations by varying the adsorption time prior to initiation of the LSV desorption step. For these results, the charge under the voltammetric peak was determined, and this is plotted in Figure 4 as a function of the

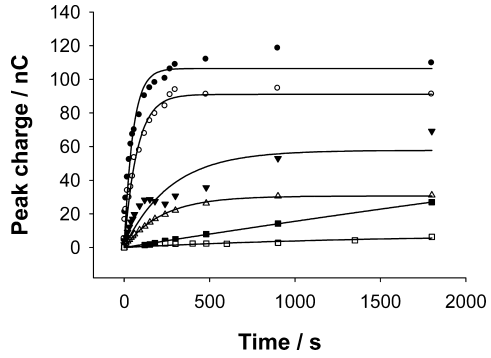

Figure 4. Kinetics of HEWL adsorption at the μITIES array at different concentrations: (□) 0.05 μM, (■) 0.1 μM, (Δ) 0.5 μM, (▼) 1.0 μM, (○) 5 μM, and (●) 10 μM HEWL, in aqueous 10 mM HCl. The solid lines (—) are the best fits to eq 2.

adsorption time and the aqueous phase concentration of HEWL. It can be seen that the charge for HEWL desorption from the μITIES array increased with the adsorption time at an applied potential of 0.95 V. The electrochemical data revealed that the adsorption of HEWL at the ITIES can be controlled by the solution concentration and the adsorption time. The charge required for desorption of the protein from the surface for any given adsorption time, Q_t, is given by[46]

$$Q_t = Q_e[1 - e^{-kCt}] \quad (2)$$

where Q_e is the equilibrium surface charge passed, k is the adsorption rate constant, C is the concentration, and t is the time, for an adsorption process under kinetic control. For the fitting of the data to this equation (Figure 4), R^2 values between 0.83 and 0.99 were obtained, while values of k obtained from the fitting increased with the aqueous phase concentration of HEWL. It is clear from Figure 4 that long adsorption times are needed in order to reach a saturation or equilibrium surface coverage at any given aqueous concentration. This may be reflected in the transport of protein molecules to the interface and their subsequent adsorption and reorientation within the adsorbed layer.[48,49] Furthermore, the possibility for structural rearrangements when the protein is present in low pH solutions was noted by Kleijn et al.[49] A purely diffusion-controlled adsorption process seems unlikely given the long times involved to reach saturation/equilibrium, together with the fact that the experiments are implemented with microinterface arrays. Under such conditions, with radial diffusion to the interface, surface saturation/equilibration should be reached quickly for a diffusion-controlled process. As discussed later, multilayer adsorption of HEWL may occur at the interfaces employed here.

Concentration Dependence. The adsorption of HEWL at the μITIES was analyzed as a function of the concentration of HEWL in the aqueous phase. As above, the analytical signal may be taken as the charge under the voltammetric peak. Figure 5 shows charge versus concentration plots for five sets of experiments in which different adsorption times were used, from 0 to 300 s, at an adsorption potential of 0.95 V. The HEWL concentration in the aqueous phase was varied between 0.05 and 10 μM.

After a period of 5 min adsorption at elevated HEWL concentrations, the amount of adsorbate at the ITIES reached a saturation point (Figure 5). However, at lower concentrations, up to ca. 1 μM, a linear dependence between the desorption

dx.doi.org/10.1021/ac203249p | Anal. Chem. 2012, 84, 2505−2511

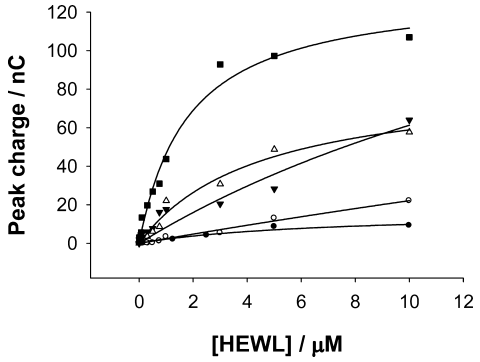

Figure 5. Concentration dependence of HEWL in 10 mM HCl determined by voltammetry following adsorption for various times: (●) 0 s, (○) 30 s, (▼) 60 s, (△) 120 s, and (■) 300 s. Experiments were performed in unstirred solutions. The organic phase was as specified in Scheme 1, Supporting Information. The solid lines (—) are guides to the eye.

charge and the concentration of HEWL in the aqueous phase exists, which can be clearly used for analytical purposes. The surface saturation charge, ca. 100 nC, is reached for the higher concentrations and longer adsorption times (Figures 4 and 5).

Sensitivity and Detection Limits. The adsorption process at the gelled μITIES array has been studied, as it may provide a means to better analytical performance via adsorptive preconcentration prior to voltammetric measurement. Peak current values plotted versus HEWL concentration show the same features as Figure 5, reaching a saturation current value of 5 nA for a maximum preconcentration time of 300 s. The linear range for the stripping current response to HEWL concentration was between 0.05 and 1 μM HEWL. As shown in Table 1, the longer preconcentration times provided a greater

Table 1. Analytical Characteristics for AdSV of HEWL at μITIES Array

preconcentration times/s	sensitivity (calibration graph slope)/nA μM^{-1}	limit of detection (LOD)/μM	linear range/ μM	rorrelation coefficient (r)
30	0.22	0.10	0−1	0.928
60	0.91	0.06	0−1	0.978
120	1.41	0.05	0−1	0.977
300	4.31	0.03	0−1	0.989

calibration graph slope (sensitivity) and lower calculated limits of detection (based on 3σ). With this AdSV approach at the μITIES array, a preconcentration time of 300 s enabled a limit of detection of 0.03 μM HEWL to be achieved, which corresponds to 0.44 μg mL^{-1}. Concentrations of 0.05 μM HEWL were detected, compared to 0.5 μM detection with CV at a similar μITIES array[28] or to even higher concentrations at ITIES.[27,31,33] This is the lowest concentration of a protein detected by electrochemistry at the ITIES to date.

Surface Coverage. In this discussion, we aim to relate the voltammetric desorption charges reported above to surface coverages for HEWL at the μITIES array. Table S-1, Supporting Information, summarizes the surface coverages for HEWL monolayers on a variety of interfaces. A variety of interfaces have been studied but not aqueous−organic interfaces. The pH values of data reported in the literature are far from the acidic conditions used in this study. Most of the surfaces employed are highly hydrophilic, with contact angle values lower than 10°. Materials such as mercury exhibit a reactive surface where the disulfide groups within the protein can react with mercury. In contrast, Su et al.[48] employed a silicon dioxide surface modified with a self-assembled monolayer of octadecyltrichlorosilane (OTS), forming a hydrophobic surface with a contact angle of 110°.[48] In the present study, the organogel phase forms one side of the adsorbing interface while HEWL is present initially in the aqueous phase under acidic conditions, where it has a charge of +17. The water contact angle of the organogel surface was determined to be ∼80°, confirming the hydrophobic property of the organic phase. Therefore, the ITIES employed here is more like the SiO_2−OTS surface than the other interfaces presented in Table S-1, Supporting Information. The monolayer surface coverage on SiO_2−OTS may be taken as that for the protein at the ITIES, noting that there are differences, such as the ITIES is charged and electrified, as well as soft, and the aqueous phase is acidic. Such differences may alter the way the protein interacts and folds/unfolds at the interface. The soft interface nature of the ITIES may lead to its being deformed or changed upon protein adsorption. Nevertheless, for now, the surface coverage of a HEWL monolayer at the μITIES is assumed to be 13 pmol cm^{-2}.

From Figures 4 and 5, the maximum charges (Q) measured can be related to surface coverage (Γ) by eq 3[46]

$$Q = z_i FA\Gamma \tag{3}$$

Taking into account the charge of the protein (z_i) at pH 2, +17,[47] the area (A) of the interface array, as patterned by the geometric area of the micropore array, 1.18×10^{-4} cm^2, and the value of the Faraday constant (F), the surface coverage can be calculated. The corresponding maximum surface coverage values determined from Figures 4 and 5 are 550 pmol cm^{-2}. If, as discussed above, we take a monolayer of adsorbed HEWL to be 13 pmol cm^{-2}, then ca. 40 monolayers of HEWL are formed at the liquid−liquid interface for a 5 min preconcentration period. Such a multilayer formation at the gelled μITIES array requires that the proteins have attractive interactions with each other. As the protein is highly charged (+17 charges), it is assumed, for now, that the organic phase supporting electrolyte anion at least partially neutralizes the protein's positive charge, so that the hydrophobic interactions arising from the exposure of the hydrophobic amino acid residues drive the attachment of the protein to the interface and to each other. The acidic nature of the aqueous phase may contribute to partial unfolding of the HEWL, exposing the internal hydrophobic regions and thus promoting multilayer adsorption at the ITIES. Furthermore, Herzog et al.[31] suggested ca. seven monolayers of hemoglobin formed at the aqueous−1,2-dichloroethane ITIES during a single CV cycle, without a preconcentration step as used here. Thus, employing a preconcentration step at an optimum applied potential for 5 min may indeed result in an order of magnitude increase in protein adsorption at the interface. As discussed by Wei et al., the nonequilibrium nature of the adsorptive process may also promote multilayer build-up of HEWL.[50] Furthermore, the formation of lysozyme multilayers on hydrophilic solid surfaces such as mica,[51] germanium crystal,[50] and $Si(Ti)O_2$[52] and on a hydrophobic surface (quartz modified with octadecyl trichlorosilane)[53] have been reported, as have the multilayer formation of two other proteins, albumin and cytochrome c, under the influence of applied potential.[54]

dx.doi.org/10.1021/ac203249p | Anal. Chem. 2012, 84, 2505−2511

CONCLUSIONS

Adsorption of the protein HEWL at miniaturized liquid−liquid interfaces has been investigated as a preconcentration strategy prior to voltammetric detection by desorption of the adsorbed material. Studies as a function of adsorption potential and adsorption time revealed that maximum protein adsorption occurs at higher positive potentials, just below the potential limit set by background electrolyte transfer. This is consistent with protein adsorbing at potentials positive of the potential of zero charge. The time dependence of the adsorption indicated that it was a slow process, associated with multilayer formation and molecular reorientations within the adsorbed film. This may be promoted by the acidic nature of the aqueous phase employed. Using a preconcentration (adsorption) time of 300 s, a limit of detection of 0.03 μM HEWL was achieved, which is the lowest concentration of protein detected by electrochemistry at the ITIES to date. The results of this study show that the limit of detection at μITIES has been improved by preconcentrating the protein at the interface. Prospective lower limits of detection may be achieved using advanced electrochemical methods in conjunction with the adsorptive preconcentration, such as differential pulse voltammetry and square wave voltammetry.

ASSOCIATED CONTENT

Supporting Information

Additional material as noted in the text (Scheme S-1, Figures S-1 to S-2, and Table S-1). This material is available free of charge via the Internet at http://pubs.acs.org.

AUTHOR INFORMATION

Corresponding Author

*E-mail: d.arrigan@curtin.edu.au. Fax: +61-8-9266-2300.

Notes

The authors declare no competing financial interest.

ACKNOWLEDGMENTS

This work was supported by Curtin University and the Western Australian Nanochemistry Research Institute. E.A.d.E. is a recipient of a Curtin Strategic International Research Scholarship. The silicon microporous membranes were a gift from Tyndall National Institute, Cork, Ireland.

REFERENCES

(1) Lehninger, A. L.; Nelson, D. L.; Cox, M. M. *Lehninger Principles of Biochemistry*; 5th ed.; W. H. Freeman: New York, 2008; p 11000.
(2) Canfield, R. E. *J. Biol. Chem.* **1963**, *238*, 2698−2707.
(3) Canfield, R. E.; Liu, A. K. *J. Biol. Chem.* **1965**, *240*, 1997−2002.
(4) Blake, C. C.; Koenig, D. F.; Mair, G. A.; North, A. C.; Phillips, D. C.; Sarma, V. R. *Nature* **1965**, *206*, 757−761.
(5) Kubiak, K.; Mulheran, P. A. *J. Phys. Chem. B* **2009**, *113*, 12189−12200.
(6) Wetter, L. R.; Deutsch, H. F. *J. Biol. Chem.* **1951**, *192*, 237−242.
(7) Shockman, G. D.; Barrett, J. F. *Annu. Rev. Microbiol.* **1983**, *37*, 501−527.
(8) Mestecky, J., Lamm, M. E., Strober, W., Bienenstock, J., McGhee, J., Mayer, L., Eds. *Mucosal Immunology*, 3rd ed.; Elsevier Academic Press: Burlington, 2005.
(9) Falchuk, K. R.; Perrotto, J. L.; Isselbacher, K. J. *Gastroenterology* **1975**, *68*, 890.
(10) Serra, C.; Vizoso, F.; Alonso, L.; Rodriguez, J. C.; Gonzalez, L. O.; Fernandez, M.; Lamelas, M. L.; Sanchez, L. M.; Garcia-Muniz, J. L.; Baltasar, A.; Medrano, J. *Breast Cancer Res.* **2002**, *4*, R16.
(11) Tahara, E.; Ito, H.; Shimamoto, F.; Iwamoto, T.; Nakagami, K.; Niimoto, H. *Histopathology* **1982**, *6*, 409−421.
(12) Mishra, O. P.; Batra, P.; Ali, Z.; Anupurba, S.; Das, B. K. *J. Trop. Pediatr.* **2003**, *49*, 13−16.
(13) Lee-Huang, S.; Huang, P. L.; Sun, Y. T.; Huang, P. L.; Kung, H. F.; Blithe, D. L.; Chen, H. C. *Proc. Natl. Acad. Sci. U.S.A.* **1999**, *96*, 2678−2681.
(14) Sava, G.; Benetti, A.; Ceschia, V.; Pacor, S. *Anticancer Res.* **1989**, *9*, 583−591.
(15) Vanysek, P.; Ramirez, L. B. *J. Chil. Chem. Soc.* **2008**, *53*, 1455−1463.
(16) Samec, Z. *Pure Appl. Chem.* **2004**, *76*, 2147−2180.
(17) Dryfe, R. A. W. *Adv. Chem. Phys.* **2009**, *141*, 153−215.
(18) Girault, H. H. *Electroanalytical Chemistry*; Bard, A. J., Zoski, C. G., Eds.; Taylor & Francis Group: New York, 2010; Vol. 23, Chapter 1, p 1−104.
(19) Arrigan, D. W. M. *Anal. Lett.* **2008**, *41*, 3233−3252.
(20) Amemiya, S.; Yang, X. T.; Wazenegger, T. L. *J. Am. Chem. Soc.* **2003**, *125*, 11832−11833.
(21) Chen, Y.; Yuan, Y.; Zhang, M. Q.; Li, F.; Sun, P.; Gao, Z.; Shao, Y. H. *Sci. China, Ser. B* **2004**, *47*, 24−33.
(22) Mendez, M. A.; Prudent, M.; Su, B.; Girault, H. H. *Anal. Chem.* **2008**, *80*, 9499−9507.
(23) Vagin, M. Y.; Malyh, E. V.; Larionova, N. I.; Karyakin, A. A. *Electrochem. Commun.* **2003**, *5*, 329−333.
(24) Vagin, M. Y.; Trashin, S. A.; Karpachova, G. P.; Klyachko, N. L.; Karyakin, A. A. *J. Electroanal. Chem.* **2008**, *623*, 68−74.
(25) Shinshi, M.; Sugihara, T.; Osakai, T.; Goto, M. *Langmuir* **2006**, *22*, 5937−5944.
(26) Osakai, T.; Yuguchi, Y.; Gohara, E.; Katano, H. *Langmuir* **2010**, *26*, 11530−11537.
(27) Scanlon, M. D.; Jennings, E.; Arrigan, D. W. M. *Phys. Chem. Chem. Phys.* **2009**, *11*, 2272−2280.
(28) Scanlon, M. D.; Strutwolf, J.; Arrigan, D. W. M. *Phys. Chem. Chem. Phys.* **2010**, *12*, 10040−10047.
(29) Trojanek, A.; Langmaier, J.; Samcova, E. J.; Samec, Z. *J. Electroanal. Chem.* **2007**, *603*, 235−242.
(30) Hartvig, R. A.; Mendez, M. A.; van de Weert, M.; Jorgensen, L.; Ostergaard, J.; Girault, H. H.; Jensen, H. *Anal. Chem.* **2010**, *82*, 7699−7705.
(31) Herzog, G.; Moujahid, W.; Strutwolf, J.; Arrigan, D. W. M. *Analyst* **2009**, *134*, 1608−1613.
(32) Herzog, G.; Kam, V.; Arrigan, D. W. M. *Electrochim. Acta* **2008**, *53*, 7204−7209.
(33) Kivlehan, F.; Lanyon, Y. H.; Arrigan, D. W. M. *Langmuir* **2008**, *24*, 9876−9882.
(34) Ellis, J. S.; Xu, S. Q.; Wang, X.; Herzog, G.; Arrigan, D. W. M.; Thompson, M. *Bioelectrochemistry* **2010**, *79*, 6−10.
(35) Gubala, V.; Harris, L. F.; Ricco, A. J.; Tan, M. X.; Williams, D. E. *Anal. Chem.* **2012**, *2*, 487−515.
(36) Fogg, A. G. *Anal. Proc.* **1995**, *32*, 433−435.
(37) Fogg, A. G.; Wang, J. *Pure Appl. Chem.* **1999**, *71*, 891−897.
(38) Kaldova, R.; Kopanica, M. *Pure Appl. Chem.* **1989**, *61*, 97−112.
(39) Pihlar, B.; Valenta, P.; Nurnberg, H. W. *Fresenius Z. Anal. Chem.* **1981**, *307*, 337−346.
(40) Guo, J. D.; Yuan, Y.; Amemiya, S. *Anal. Chem.* **2005**, *77*, 5711−5719.
(41) Osakai, T.; Kakutani, T.; Senda, M. *J. Electrochem. Soc.* **1987**, *134*, C520−C520.
(42) Zazpe, R.; Hibert, C.; O'Brien, J.; Lanyon, Y. H.; Arrigan, D. W. M. *Lab Chip* **2007**, *7*, 1732−1737.
(43) Strutwolf, J.; Scanlon, M. D.; Arrigan, D. W. M. *Analyst* **2009**, *134*, 148−158.
(44) Scanlon, M. D.; Herzog, G.; Arrigan, D. W. M. *Anal. Chem.* **2008**, *80*, 5743−5749.
(45) Berduque, A.; Scanlon, M. D.; Collins, C. J.; Arrigan, D. W. M. *Langmuir* **2007**, *23*, 7356−7364.
(46) Wang, J. *Analytical Electrochemistry*, 2nd ed.; Wiley-VCH: New York, 2000.

(47) Kuramitsu, S.; Hamaguchi, K. *J. Biochem.* **1980**, *87*, 1215−1219.
(48) Su, T. J.; Green, R. J.; Wang, Y.; Murphy, E. F.; Lu, J. R.; Ivkov, R.; Satija, S. K. *Langmuir* **2000**, *16*, 4999−5007.
(49) Kleijn, J. M.; Barten, D.; Stuart, M. A. C. *Langmuir* **2004**, *20*, 9703−9713.
(50) Wei, T.; Kaewtathip, S.; Shing, K. *J. Phys. Chem. C* **2009**, *113*, 2053−2062.
(51) Kim, D. T.; Blanch, H. W.; Radke, C. J. *Langmuir* **2002**, *18*, 5841−5850.
(52) Ball, V.; Ramsden, J. J. *Colloids Surf., B* **2000**, *17*, 81−94.
(53) Schmidt, C. F.; Zimmermann, R. M.; Gaub, H. E. *J. Biophys.* **1990**, *57*, 577−588.
(54) Brusatori, M. A.; Tie, Y.; Van Tassel, P. R. *Langmuir* **2003**, *19*, 5089−5097.